

## Sensor signal processing

**Adaptive Threshold for Zero-Velocity Detector in ZUPT-Aided Pedestrian Inertial Navigation**

Yusheng Wang\* and Andrei M. Shkel\*\*

*The authors are with the Department of Mechanical and Aerospace Engineering, University of California, Irvine, CA 92697 USA**\*Student Member, IEEE**\*\*Fellow, IEEE*

Manuscript received June 27, 2019; revised September 11, 2019; accepted October 4, 2019. Date of publication October 7, 2019; date of current version November 20, 2019.

**Abstract**—We present a study on the adaptive threshold of the zero-velocity detector, which enables the detector to adjust to gait patterns with different speeds, from as low as walking with 80 steps per minute to as high as running with 160 steps per minute, without any tuning of design parameters during the navigation. This approach enables the zero-velocity update (ZUPT)-aided navigation algorithm to work properly with time-varying speed in a single navigation process. A Bayesian-based approach was applied to determine the adaptive threshold in the likelihood ratio test with a uniform prior information and time-varying cost function. The position error in a velocity-changing navigation scenario was demonstrated to be reduced by 12 times after applying the adaptive threshold instead of a fixed threshold.

**Index Terms**—Sensor signal processing, adaptive threshold, pedestrian inertial navigation, zero-velocity detector, zero-velocity update (ZUPT).

**I. INTRODUCTION**

Pedestrian inertial navigation has been made possible with a rapid development of microelectromechanical systems based inertial measurement units (IMUs), which are achieving better noise characteristics, lighter weight, smaller size, and also lower cost [1]. However, errors in IMU readouts cause navigation errors, which accumulate approximately proportional to the time cubed and exceed a meter of error within only a few seconds of navigation with consumer grade IMUs and about 20 s with tactical grade IMUs [2].

Zero-velocity update (ZUPT)-aided navigation algorithm [3] is one of the commonly used compensation mechanisms for pedestrian inertial navigation. It takes advantage of the stationary state of the foot during the stance phase and feeds the zero-velocity information (pseudomeasurement) into Kalman filter (KF) to compensate for IMU errors (see Fig. 1). Hours of navigation has been demonstrated with ZUPT-aided inertial navigation algorithm with navigation errors less than 10 m [5]. To implement the algorithm, a zero-velocity detector is necessary to determine if the IMU is stationary or not by comparing test statistics to a threshold.

However, different gait patterns lead to different gait dynamics, and as a result, different thresholds are required. A variety of threshold tuning methods have been reported. Some tuned the threshold empirically in an ad-hoc manner [6], [7]. Others adjusted the parameters based on the period of gait cycle (or equivalently, the walking speed) obtained by presetting the walking speed or Fourier transform [8], [9]. Sensor-fusion techniques have been also proposed to tune the parameter [10], [11]. More recently, machine learning was explored to classify the motion first, and then assign the threshold accordingly [12], [13]. All these techniques either achieved adaptive threshold by increasing complexity of the system, or had some assumptions on the level of gait speed. This letter intends to fill the gap by developing an adaptive threshold in ZUPT detection without increasing complexity of the system.

Corresponding author: Yusheng Wang (e-mail: yushengw@uci.edu).

Associate Editor: G. Langfelder.

Digital Object Identifier 10.1109/LSENS.2019.2946129



Fig. 1. Foot-mounted IMU used in ZUPT-aided pedestrian inertial navigation. A near-tactical grade VN-200 IMU was rigidly mounted above the forefoot of the boot by three-dimensional-printed fixtures for better navigation accuracy [4].

**II. ZERO-VELOCITY DETECTOR**

A zero-velocity detector can be mathematically expressed as a binary hypothesis testing problem, where the detector can choose between the two hypotheses:  $H_0$  and  $H_1$ , where  $H_0$  corresponds to the case where the IMU is moving, while  $H_1$  corresponds to the case where the IMU is stationary. A common approach is to apply the Neyman–Pearson theorem and compare the likelihood ratio with some predefined threshold  $\gamma$  [14]: choose  $H_1$  if

$$L(\mathbf{z}_n) = \frac{p(\mathbf{z}_n | H_1)}{p(\mathbf{z}_n | H_0)} > \gamma \quad (1)$$

where  $\mathbf{z}_k = \{\mathbf{y}_k\}_{k=n}^{n+N-1}$  is the  $N$  consecutive IMU readouts between time index  $n$  and  $n + N - 1$ , and  $L(\cdot)$  is the likelihood ratio of probability of the measurement.

Stance hypothesis optimal detector is one of the most commonly used zero-velocity detector [15]. This detector is based on the fact

that during the stance phase, the magnitude of the specific force that the IMU is experiencing is equal to the gravity, and the angular rate of the IMU is zero. Since the accurate dynamics of human gait is complicated, if not unavailable, many parameters that determine the probability density functions (PDF) of observations are unknown [16]. Therefore, the unknown parameters are replaced with their maximum likelihood (ML) estimates, and this method is the generalized likelihood ratio test (GLRT) [17]. The test statistics can be expressed as

$$\begin{aligned} L'_{\text{ML}}(z_n) &= -\frac{2}{N} \log(L_{\text{ML}}(z_n)) \\ &= \frac{1}{N} \sum_{k=n}^{n+N-1} \frac{1}{\sigma_a^2} \| \mathbf{y}_k^a - g \frac{\bar{\mathbf{y}}^a}{\| \bar{\mathbf{y}}^a \|} \|^2 + \frac{1}{\sigma_\omega^2} \| \mathbf{y}_k^\omega \|^2 \quad (2) \end{aligned}$$

where  $\mathbf{y}_k^a$  and  $\mathbf{y}_k^\omega$  are the accelerometer and the gyroscope readouts at time index  $k$ , respectively,  $\bar{\mathbf{y}}^a$  is the averaged value of the  $N$  consecutive accelerometer readouts,  $\sigma_a$  and  $\sigma_\omega$  are related to the white noise level of the accelerometer and the gyroscope, and  $g$  is the gravity.

We can then state the GLRT as: choose  $H_1$  if

$$L'_{\text{ML}}(z_n) < \gamma' \quad (3)$$

where  $\gamma'$  is the threshold to be determined.

### III. ADAPTIVE THRESHOLD DETERMINATION

For different gait patterns, the distributions of  $z_n$  are also different, and therefore different thresholds are needed. In this section, we derive an adaptive threshold based on time dependent prior information and cost function.

There are three general goals of adaptive threshold.

- 1) Limit the probability of false alarm. False alarm happens if the detector determines the IMU is stationary while the foot is actually moving. False alarm will cause KF to erroneously set the velocity close to zero, which greatly degrade the results of navigation.
- 2) Minimize the probability of miss detection. Stance phase is the time period when zero-velocity information can be utilized to suppress the navigation error growth. Miss detection will reduce the chance of compensation, therefore increase the overall navigation error.
- 3) Adjust the threshold parameters automatically to fit different gait dynamics and maintain a proper amount of zero-velocity updates.

Fig. 2 shows a typical test statistic  $L'_{\text{ML}}(z_n)$  with different gait dynamics. There are six different gait dynamics shown in Fig. 2, corresponding to walking at the pace of 80, 90, 100, 110, and 120 steps per minute, and running at the pace of 160 steps per minute, respectively. High statistic indicates that the IMU is moving while a lower value shows that the IMU is close to a stationary state. Fig. 2 shows that the test statistic is around 100 when the foot is actually stationary (represented by the time period between the six movements). The red-dashed lines are the averaged values of test statistics during the stance phase related to different gait dynamics, ranging from the lowest of  $4 \times 10^4$  to the highest of  $6 \times 10^5$ . The purpose of the adaptive threshold is to capture differences caused by different walking and running paces and patterns. Note that these values are much higher than the test statistic when the foot is stationary on the floor, indicating that the foot is not absolutely stationary even during the stance phase. As a result, an excessive use of zero-velocity update will cause degradation to the overall navigation accuracy [18].

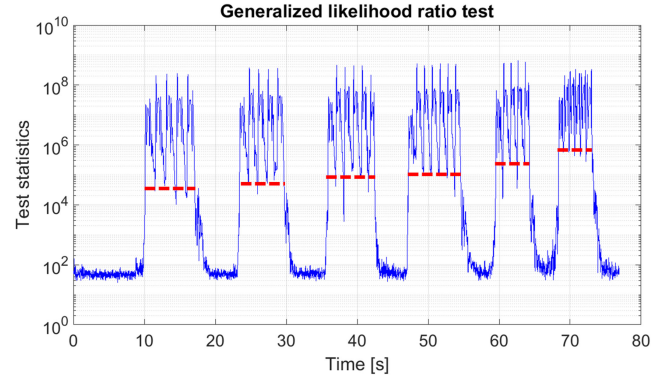


Fig. 2. Blue line is a typical test statistic for different walking and running paces. The red-dashed lines are the test statistic levels of stance phase with different gait paces.

The Bayesian likelihood ratio test states that the threshold can be expressed as

$$\gamma = \frac{p(H_0)}{p(H_1)} \cdot \frac{c_{10} - c_{00}}{c_{01} - c_{11}} \quad (4)$$

where  $p(H_0)/p(H_1)$  is the prior probability of the hypotheses,  $c_{00}$ ,  $c_{11}$ ,  $c_{10}$ , and  $c_{01}$  are the cost functions of correctly detecting the swing phase, correctly detecting the stance phase, a false alarm, and a miss detection, respectively. We assume a uniform prior probability and zero cost function for correct detection. Thus, the threshold is only the ratio of the cost function of false alarm and miss detection.

The miss detection is the case where the detector determines that the IMU is moving during the stance phase. The associated cost is time-dependent by its nature, since the navigation error accumulates as a polynomial with respect to time without any error suppression [19]. The order of the polynomial is related to many factors, such as the time duration, IMU noise level, and dynamics of motion. Therefore, we believe that it is proper to assume a polynomial cost function for miss detection instead of an exponential one reported in [8]. On the other hand, the cost of a false alarm is relatively time-independent compared to a miss detection [8]. Therefore, we can assume a constant cost for the false alarm and a polynomial cost for miss detection. We define the ratio of the cost of a false alarm to the cost of a miss detection to be

$$\gamma = \frac{c_{10}}{c_{01}} = \alpha_1 \cdot \Delta t^{-\theta_1} \quad (5)$$

where  $\Delta t$  is the time difference between the previous ZUPT and the current time step, and  $\alpha_1$  and  $\theta_1$  are design parameters to be decided. The threshold  $\gamma'$  can be expressed as

$$\begin{aligned} \gamma' &= -\frac{2}{N} \log(\gamma) = -\frac{2}{N} (\log(\alpha_1) - \theta_1 \cdot \log(\Delta t)) \\ &\triangleq \theta \cdot \log(\Delta t) + \alpha. \quad (6) \end{aligned}$$

$\gamma'$  is small immediately after detection of the last stance phase since  $\Delta t$  is small. The physical interpretation is that the probability of detecting another stance phase is low, according to (6), since we do not expect two stance phases very close to each other.

Another advantage of polynomial cost can be shown from (6). Note that (6) would be in the form of  $\theta \cdot \Delta t + \alpha$ , if exponential cost were to be used. For normal gait patterns, the range of  $\Delta t$  is typically around 1 s. The slope of  $\log(\Delta t)$ , which is associated with the polynomial cost, is similar to that of  $\Delta t$ , which is in turn associated with the exponential cost, when  $\Delta t$  is around 1 s, but the slope is much larger

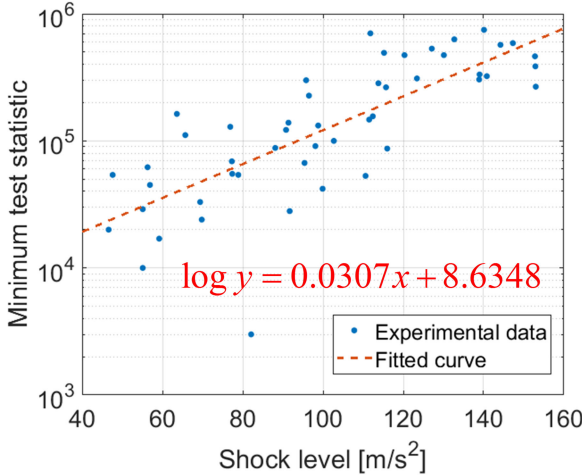


Fig. 3. Relation between the shock level and the minimum test statistics in the same gait cycle. The dots correspond to data from different gait cycles and the red-dashed line is the fitted curve.

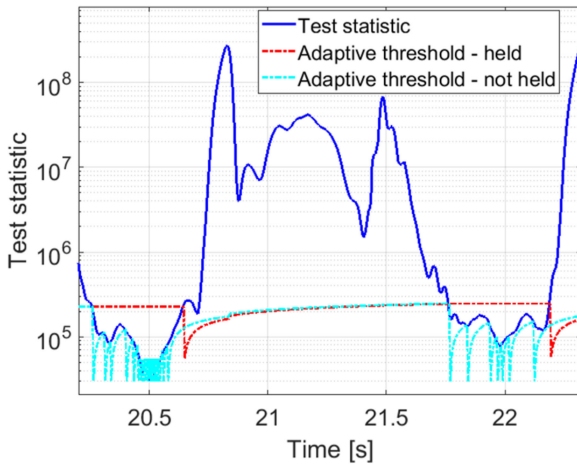


Fig. 4. Comparison of the adaptive thresholds with and without an artificial holding.

if  $\Delta t$  is smaller than 1 s. Therefore, a similar performance of stance phase detection could be expected with a better robustness against false alarm in between the two stance phases. The threshold  $\gamma'$  will increase at a speed defined by  $\theta$  as  $\Delta t$  increases, and  $\alpha$  defines the overall level of the threshold. Ideally,  $\theta$  would be defined such that  $\gamma'$  increases to the level of the test statistic during the stance phase (indicated by the red-dashed lines in Fig. 2), when the next stance phase would actually start. This requires an estimation of the level of the test statistic during the stance phase, which is directly related to the gait frequency. In this letter, instead of predefining the gait frequency as in [8], which is unrealistic in real navigation applications, or applying the Fourier transform to extract the gait frequency as in [9], whose response to frequency change is slow, we propose to take advantage of the shock level that the IMU experiences during the heel strike as an indicator to estimate the real-time gait frequency.

As the step pace increases, the minimum test statistics increases, as well as the shock level that the IMU experiences during the heel strike. The relation between the shock level and the minimum test statistics is shown in Fig. 3. The dots correspond to data from different gait cycles and the red-dashed line is the fitted curve. An exponential formula can be used to approximate the relation, and the parameter  $\theta$  in (6) can be

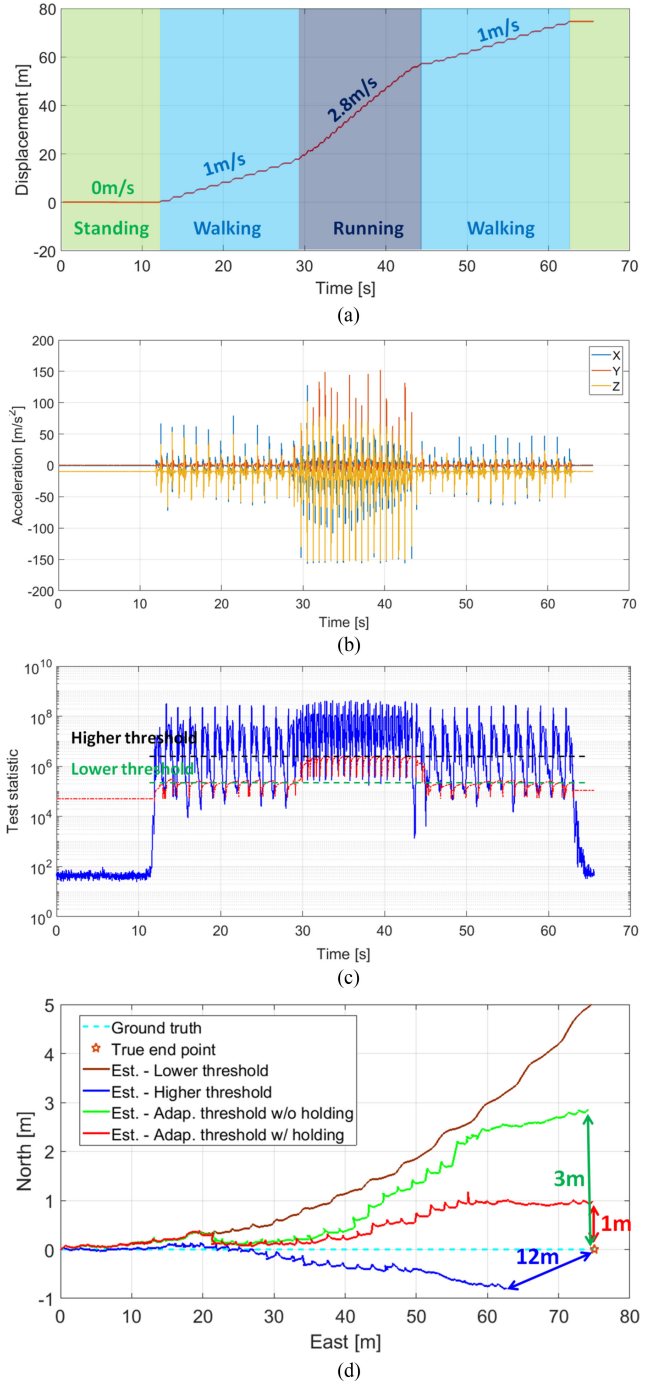


Fig. 5. Position propagation, specific force of the IMU, GLRT, and the navigation results of the experiment. Note that the x- and y-axis scalings in (d) are different. (a) Position propagation. (b) IMU specific force. (c) Test statistic and adaptive threshold. (d) Estimated trajectory comparison.

defined as

$$\theta = \epsilon \cdot \exp(0.0307 \times \text{Shock} + 8.6348) \quad (7)$$

where Shock is the shock level during the heel strike,  $\epsilon$  is the parameter that can be adjusted to achieve a proper length of the stance phase, and it is set to be 3.5 in this letter, and  $\alpha$  can also be adjusted accordingly.

Advantages of using shock level during the heel strike to extract gait frequency include the following.

- 1) No priori knowledge of the gait frequency is needed.
- 2) Ability to track continuously changing gait frequency with faster response than Fourier transform.
- 3) Shock level can be directly measured and the required computational power is much lower than machine learning methods.

To ensure that enough zero-velocity updates could be implemented to suppress the navigation error, we artificially hold the threshold  $\gamma'$  until it becomes smaller than the test statistic again, instead of allowing it to drop back as (6) indicates. The effect of the holding is shown in Fig. 4. The artificial holding enables us to detect the whole stance phase instead of just some time instances in the stance phase.

#### IV. EXPERIMENTAL VERIFICATION

Experiments have been conducted to verify the effects of the adaptive threshold. A straight trajectory of 75 m was used in the experiment. IMU was rigidly mounted above the forefoot (see Fig. 1) and the sampling rate was 200 Hz. During the navigation, the agent first stood for about 12 s, then walked at a pace of 80 steps per minute for about 15 s. It was followed by running at a pace of 160 steps per minute for about 15 s and walking for another 20 s. At last, the agent stood for about 5 s. The position propagation, accelerometer readouts, GLRT, and the navigation results are presented in Fig. 5. Fig. 5(a) shows the velocity difference between walking and running. Fig. 5(b) shows the specific force of the IMU. A much higher shock level of about  $150 \text{ m/s}^2$  during running was observed, exceeding the level of about  $50 \text{ m/s}^2$  during walking. Fig. 5(c) shows the test statistics (solid blue line) and the adaptive threshold (red-dashed line). The minimum test statistics for walking and running were about  $2 \times 10^5$  (lower threshold) and  $2 \times 10^6$  (higher threshold), respectively. The adaptive threshold successfully captured the changes of dynamics. Fig. 5(d) shows the comparison of estimated trajectories with the adaptive threshold with and without artificial holding, with the lower fixed threshold shown in Fig. 5(c), and with the higher fixed threshold shown in Fig. 5(c). The stance phase during running could not be detected with lower threshold. Thus, the estimated trajectory drifted away after the agent started running. Too many zero-velocity updates were imposed during walking with higher threshold. Therefore, the estimated trajectory was shorter than the ground truth, causing a large navigation error of 12 m. The navigation error was reduced to about 1 m with the adaptive threshold.

#### V. CONCLUSION

In this letter, we implemented an adaptive threshold for the ZUPT-aided pedestrian inertial navigation, enabling ZUPT-aided pedestrian inertial navigation with continuously changing gait frequency. The method was based on the Bayesian approach and the dynamics relating the shock level of the IMU and the test statistic during the stance phase. With the adaptive threshold implemented, the navigation error was experimentally demonstrated to be reduced by 12 times compared to a fixed threshold, with only a marginal increase in the system complexity to extract the shock level during the gait cycle.

#### ACKNOWLEDGMENT

This work was performed under the following financial assistance award: 70NANB17H192 from U.S. Department of Commerce, National Institute of Standards and Technology. All the work was conducted in the MicroSystems Laboratory at University of California, Irvine.

#### REFERENCES

- [1] M. Perlmutter and L. Robin, "High-performance, low cost inertial MEMS: A market in motion!" in *Proc. IEEE/ION Position, Location Navigat. Symp.*, Myrtle Beach, SC, USA, Apr. 23–26, 2012, pp. 225–229.
- [2] M. Ma, Q. Song, Y. Li, and Z. Zhou, "A zero velocity intervals detection algorithm based on sensor fusion for indoor pedestrian navigation," in *Proc. IEEE Inf. Technol., Netw., Electron. Autom. Control Conf.*, Chengdu, China, Dec. 15–17, 2017, pp. 418–423.
- [3] E. Foxlin, "Pedestrian tracking with SHOE-mounted inertial sensors," *IEEE Comput. Graph. Appl.*, vol. 25, no. 6, pp. 38–46, Nov./Dec. 2005.
- [4] Y. Wang, S. Askari, and A. M. Shkel, "Study on mounting position of IMU for better accuracy of ZUPT-aided pedestrian inertial navigation," in *Proc. IEEE Int. Symp. Inertial Sensors Syst.*, Naples, FL, USA, Apr. 1–5, 2019, pp. 1–4.
- [5] M. Laverne, M. George, D. Lord, A. Kelly, and T. Mukherjee, "Experimental validation of foot to foot range measurements in pedestrian tracking," in *Proc. ION GNSS Conf.*, Portland, OR, USA, Sep. 19–23, 2011.
- [6] I. Skog, J.-O. Nilsson, and P. Handel, "Evaluation of zero-velocity detectors for foot-mounted inertial navigation systems," in *Proc. IEEE Int. Conf. Indoor Positioning Indoor Navigation*, Zurich, Switzerland, Sep. 15–17, 2010, pp. 1–6.
- [7] X. Meng, Z.-Q. Zhang, J.-K. Wu, W.-C. Wong, and H. Yu, "Self-contained pedestrian tracking during normal walking using an inertial/magnetic sensor module," *IEEE Trans. Biomed. Eng.*, vol. 61, no. 3, pp. 892–899, Mar. 2014.
- [8] J. Wahlstrom, I. Skog, F. Gustafsson, A. Markham, and N. Trigoni, "Zero-velocity detection—A Bayesian approach to adaptive thresholding," *IEEE Sensors Lett.*, vol. 3, no. 6, pp. 1–4, Jun. 2019.
- [9] X. Tian, J. Chen, Y. Han, J. Shang, and N. Li, "A novel zero velocity interval detection algorithm for self-contained pedestrian navigation system with inertial sensors," *Sensors*, vol. 16, no. 10, 2016, Art. no. 1578.
- [10] P. Stromback *et al.*, "Foot-mounted inertial navigation and cooperative sensor fusion for indoor positioning," in *Proc. ION Int. Tech. Meeting*, San Diego, CA, USA, Jan. 25–27, 2010, pp. 89–98.
- [11] M. Ma, Q. Song, Y. Li, and Z. Zhou, "A zero velocity intervals detection algorithm based on sensor fusion for indoor pedestrian navigation," in *Proc. IEEE Inf. Technol., Netw., Electron. Autom. Control Conf.*, Chengdu, China, Dec. 15–17, 2017, pp. 418–423.
- [12] B. Wagstaff, V. Peretroukhin, and J. Kelly, "Improving foot-mounted inertial navigation through real-time motion classification," in *Proc. IEEE Int. Conf. Indoor Positioning Indoor Navigat.*, Sapporo, Japan, Sep. 18–21, 2017, pp. 1–8.
- [13] R. Zhang, H. Yang, F. Hofflinger, and L. M. Reindl, "Adaptive zero velocity update based on velocity classification for pedestrian tracking," *IEEE Sensors J.*, vol. 17, no. 7, pp. 2137–2145, Apr. 2017.
- [14] H. L. Van Trees, *Detection, Estimation, and Modulation Theory, Part I: Detection, Estimation, and Linear Modulation Theory*, 2nd ed. Hoboken, NJ, USA: Wiley, 2004.
- [15] I. Skog, P. Handel, J.-O. Nilsson, and J. Rantakokko, "Zero-velocity detection—An algorithm evaluation," *IEEE Trans. Biomed. Eng.*, vol. 57, no. 11, pp. 2657–2666, Nov. 2010.
- [16] Y. Wang, A. Chernyshoff, and A. M. Shkel, "Error analysis of ZUPT-aided pedestrian inertial navigation," in *Proc. IEEE Int. Conf. Indoor Positioning Indoor Navigat.*, Nantes, France, Sep. 24–27, 2018, pp. 206–212.
- [17] O. Zeitouni, J. Ziv, and N. Merhav, "When is the generalized likelihood ratio test optimal?" *IEEE Trans. Inf. Theory*, vol. 38, no. 5, pp. 1597–1602, Sep. 1992.
- [18] J.-O. Nilsson, I. Skog, and P. Handel, "A note on the limitations of ZUPTs and the implications on sensor error modeling," in *Proc. IEEE Int. Conf. Indoor Positioning Indoor Navigat.*, Sydney, Australia, Nov. 13–15, 2012.
- [19] Y. Wang, D. Vatanparvar, A. Chernyshoff, and A. M. Shkel, "Analytical closed-form estimation of position error on ZUPT-augmented pedestrian inertial navigation," *IEEE Sensors Lett.*, vol. 2, no. 4, pp. 1–4, Dec. 2018.